crystals

MDPI

Article

Effect of Dopants on Laser-Induced Damage Threshold of $ZnGeP_2$

Nikolay Yudin [1,*], Mikhail Zinoviev [1], Vladimir Kuznetsov [2], Elena Slyunko [1], Sergey Podzvalov [1], Vladimir Voevodin [1], Alexey Lysenko [1], Andrey Kalsin [1], Leyla Shaimerdenova [1], Houssain Baalbaki [1] and Vera Kalygina [1]

[1] Laboratory for Radiophysical and Optical Methods of Environmental Studies, National Research Tomsk State University, 634050 Tomsk, Russia
[2] Institute of High Current Electronics, Akademichesky ave. 2/3, 634055 Tomsk, Russia
* Correspondence: rach3@yandex.ru; Tel.: +7-996-938-71-32

Abstract: The effect of doping Mg, Se, and Ca by diffusion into $ZnGeP_2$ on the optical damage threshold at a wavelength of 2.1 μm has been studied. It has been shown that diffusion-doping with Mg and Se leads to an increase in the laser-induced damage threshold (LIDT) of a single crystal (monocrystal), $ZnGeP_2$; upon annealing at a temperature of 750 °C, the damage threshold of samples doped with Mg and Se increases by 31% and 21% from 2.2 ± 0.1 J/cm^2 to 2.9 ± 0.1 and 2.7 ± 0.1 J/cm^2, respectively. When $ZnGeP_2$ is doped with Ca, the opposite trend is observed. It has been suggested that the changes in the LIDT depending on the introduced impurity by diffusion can be explained by the creation of additional energy dissipation channels due to the processes of radiative and fast non-radiative relaxation through impurity energy levels, which further requires experimental confirmation.

Keywords: single crystal; $ZnGeP_2$; laser-induced damage threshold; crystal structure

Citation: Yudin, N.; Zinoviev, M.; Kuznetsov, V.; Slyunko, E.; Podzvalov, S.; Voevodin, V.; Lysenko, A.; Kalsin, A.; Shaimerdenova, L.; Baalbaki, H.; et al. Effect of Dopants on Laser-Induced Damage Threshold of $ZnGeP_2$. *Crystals* **2023**, *13*, 440. https://doi.org/10.3390/cryst13030440

Academic Editor: Evgeniy N. Mokhov

Received: 13 September 2022
Revised: 16 February 2023
Accepted: 28 February 2023
Published: 3 March 2023

1. Introduction

Today, nonlinear optical frequency converters are considered as efficient coherent radiation sources in the mid-IR wavelength range equally with CO_2, CO, and HF gas lasers. $ZnGeP_2$ (ZGP) is a high-efficient nonlinear crystal for parametric oscillations in mid-IR radiation.

The ternary compound, ZGP, crystallizing in the chalcopyrite structure with a 42 m point-group [1,2] has a high thermal conductivity of 0.35 W/cm·K and a birefringence sufficient for phase-matching [3–5]. These advantages have made ZGP an effective material for non-linear optical devices and high-power optical parametric oscillators (OPO). The maximum potential of nonlinear optical $ZnGeP_2$ crystals is realized in OPO that convert laser radiation with a wavelength near 2.1 μm into radiation tunable in the region of 3–8 μm [6,7].

The authors in [8–15] reported that OPOs based on ZnGeP2 crystals generate radiation (with optical conversion efficiency of ~70%) with an average power of ~200 W or pulsed energy up to 200 mJ at pulse repetition rates from 1 Hz up to 100 kHz and pulse duration between 15–50 ns. However, as mentioned in [9–12], the reliable operation of these systems, under these extreme generation modes, is limited by the effects of thermal accumulation and optical damage, which limits the operating time of the systems in the range of several seconds. In this regard, these highly efficient sources of coherent radiation in the mid-IR range are only used when the powerful short-term pulse trains are required.

The problem of ZGP optical damage at a wavelength of ~2.1 μm and the technological methods that allow an increase in the optical damage threshold were studied. In particular, a direct correlation of the optical damage threshold on the technology of growth and the optical quality of crystals was illustrated in [16,17]. Comprehensive studies were carried out on the effect of the polishing quality of the working surfaces of the crystal on the LIDT of ZGP [17,18]. In [18], it was shown that the complete removal of the near-surface

cracked layer during polishing allows an almost twofold increase in the optical damage threshold and in [17], it was shown that the irregularities of the polished surface peaks and troughs are seeds of hetero-homogeneities, which cause optical damage due to field effects. In [19], an angstrom level of surface roughness was obtained using magnetorheological polishing of the ZGP crystal surface. It has been shown that the LIDT at the angstrom level of surface roughness is determined by the concentration of dislocations or volume defects "outcropping" on polished surfaces and not by the level of surface roughness. In [20], it was shown that the measured damage threshold for ZGP samples with an antireflection coating are much lower than for uncoated ones. While in [18], it was shown that the optical damage threshold is increased by two times when the deposition of anti-reflection interference coatings are used. Studies [21–23] were carried out to determine the composition and parameters of the anti-reflection coating that have an effect on the optical damage threshold of the ZGP crystal. Dynamic visualization of the damage, which occurs using laser radiation at a wavelength of 2.1 μm in the ZGP volume, showed that the temperature sharply increases in the emerging path inside the nonlinear optical element [24,25]. In [17], a significant correlation of the LIDT of ZGP on the crystal temperature was observed. As the temperature decreases from 0 °C to −60 °C, the energy density of the threshold is sharply increased by 1.5 times. An increase in the LIDT with a decrease in the temperature of ZGP is demonstrated by the dependence of the temperature of the phonon occupation numbers, which together with optical quanta take part in indirect transitions to the impurity level from the valence band.

In [19], an increase in the damage threshold of ZGP with a decrease in the duration of pump radiation pulses was explained by the thermal nature of the breakdown by nanosecond pulses due to anomalous absorption in the mid-IR range [20,21]. In [16], it was reported that a decrease in the dislocation concentration inside a ZGP sample by an order of magnitude allows an increase in the LIDT by more than three times.

Thus, the responsible mechanisms for the optical damage of ZGP by nanosecond pulses of laser radiation with a wavelength of 2.1 μm are not entirely clear. Currently, the technological methods of synthesis, growth, and post-growth processing that contribute to the increase in the LIDT of ZGP are actively studied.

The doping is a quite evident way to increase the LIDT of optical materials and this approach was well-studied in the 70–80s of the 20th century. Today, research is being actively carried out on doping various optical and nonlinear materials to modify their optical, mechanical, and nonlinear properties, and to increase their optical damage threshold.

In [26], an increase in the optical damage threshold of GaSe by five times, a decrease in absorption in the mid-IR and THz ranges by three times, neutralization of two-photon absorption, and a significant increase in the nonlinearity of the crystal due to controlled doping during growth with Te, Al, Er, and In were achieved. In [27], the mechanisms of optical damage of Ga-As-Sb-S chalcogenide glass doped with Tm ions under the action of femtosecond laser radiation were studied. In [28], the results of the studies of the LIDT of sapphire and Ti:sapphire under the action of pulsed laser radiation in the visible and IR ranges with a variable pulse duration from fs to ns are presented. An explanation for the increase in the LIDT of Ti-doped sapphire samples can be due to the additional energy dissipation channels during doping by radiative and fast non-radiative relaxation processes.

Despite the existing successful experience in increasing the LIDT of crystals by modifying their properties as a result of controlled doping by atoms of various chemical elements, there are no devoted works for studying the effect of diffusion-doping with various chemical elements on the LIDT of ZGP. In [29], ZGP was doped with the chemical element Mn during which a new ferromagnetic material, $Zn_xMn_{1-x}GeP_2$, was obtained; however, studies on the effect of doping on the optical damage threshold have not been carried out. In addition, studies were carried out in [30] on the effect of diffusion-doping with a Cu impurity on the electrical properties of ZGP crystals. As shown by these studies, doping Cu by diffusion-annealing is an effective way to vary the concentration of holes within

10^{12}–10^{16} cm^{-3} in ZGP due to the acceptor nature of Cu defects; however, studies of the doping effect on the LIDT have also not been carried out.

The aim of the work presented here is to elucidate the effect of diffusion-doping with such chemical elements as Mg, Se, and Ca on the optical damage threshold of ZGP when it is radiated using a wavelength of 2.1 μm.

2. Sputtering Technique

For studies, a single crystal ZGP was used from which 8 samples were cut with (100) orientation and dimensions 5 × 5 × 2.45 mm^3. Polishing of the working surfaces of the studied samples was carried out on a 4-PD-200 polishing and finishing machine. The initial processing of the working surfaces of all samples consisted of polishing on a cambric-polishing pad using the synthetic diamond powder, ACM 0.5/0 (average grain size 270 nm), followed by polishing with the synthetic diamond powder, ACM 0.25/0.

Mg, Se, and Ca were thermally sputtered onto the pre-polished faces of the samples (the thickness of the sprayed film was 1 μm). After that, the ZGP samples with deposited films and two control samples without deposition were annealed in a sealed evacuated ampoule into which a weighed amount of ZGP powder was added at temperatures of 650 °C for one set of samples and at 750 °C for another similar set for 180 h. After diffusion-doping, the working surfaces of the test samples were re-polished according to the method described above.

The optical damage threshold was measured for the processed ZGP samples. The radiation source was a Ho:YAG laser, generating radiation at a wavelength of 2.097 μm and pumped by a CW thulium fiber laser. The Ho:YAG laser operated in the active Q-switched mode with a pulse duration, τ, of 35 ns and a pulse repetition rate of 10 kHz. In all the experiments, the laser beam diameter, d, at the input aperture of the studied sample was 350 ± 10 μm at the e^{-2} level of maximum intensity. The maximum average radiation power generated using the Ho:YAG laser was 20 W.

Figure 1 shows the experimental setup scheme. An attenuator consisting of a half-wave plate (λ/2) and a polarizing prism (BSC) was used to change the power of the incident laser radiation. Additionally, a Faraday isolator (F.I.) was used to prevent the reflected radiation from entering the laser and an uncontrolled change in the parameters of the acting radiation. Before each experiment, the average laser power (P_{av}) was measured using an Ophir power meter (P.M.).

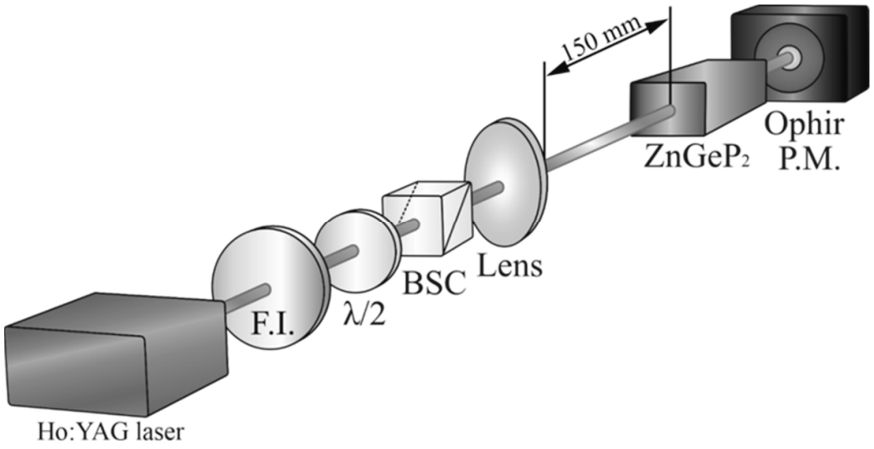

Figure 1. Optical scheme of the experimental setup: 1—Ho:YAG laser, F.I.—Faraday insulator, λ/2—half–wave plate, BSC—Glan prism, P.M.—Ophir power meter.

In accordance with the international standard, ISO11146 [31], the laser radiation energy density was calculated by the following equation:

$$W = 8\,P_{av}/\left(f\pi d^2\right), \quad (1)$$

where d is the laser beam diameter and f is the pulse repetition rate.

The "R-on-1" method was used to determine the optical damage threshold. The R-on-1 method requires less space on the sample surface in comparison with the S-on-1 method, which is used with a limited aperture although is considered rougher [32]. The brief of this method is that the laser radiation with a sequential increase in its intensity irradiates each individual area of the sample until an optical damage takes place or a pre-determined value of energy density is reached. The study was conducted with an exposure duration (τ_{ex}) of 5 s. The studied sample was exposed to packets of laser pulses with a fixed level of energy density where no damage was recorded on the surface of the crystals. Subsequently, the level of energy density was raised with a step of ~0.1 J/cm^2. When a visible damage appeared on one of the surfaces of the nonlinear sample, the experiment was stopped. Next, the sample was moved using a two-coordinate shift in height or width by 0.5 mm; the experiment was repeated 5 times. The probability of optical damage was obtained by plotting the cumulative probability as a function of the energy density of the optical damage. The optical breakdown threshold (W0d) was considered to be the energy density corresponding to the approximation of the probability of optical breakdown to zero.

Further, the specific conductivity of the ZGP samples was measured by the van der Pauw method [33].

The transmission of the studied samples in the wavelength range of 0.6–12 μm was recorded using a Shimadzu UV-3600 spectrophotometer and a Simex Fourier spectrophotometer.

3. Experimental Results and Discussion

The measurements of the optical damage threshold of ZGP samples annealed at temperatures of 650 °C and 750 °C without doping and with doping with Mg, Se, and Ca using the R-on-1 method are shown in Figure 2.

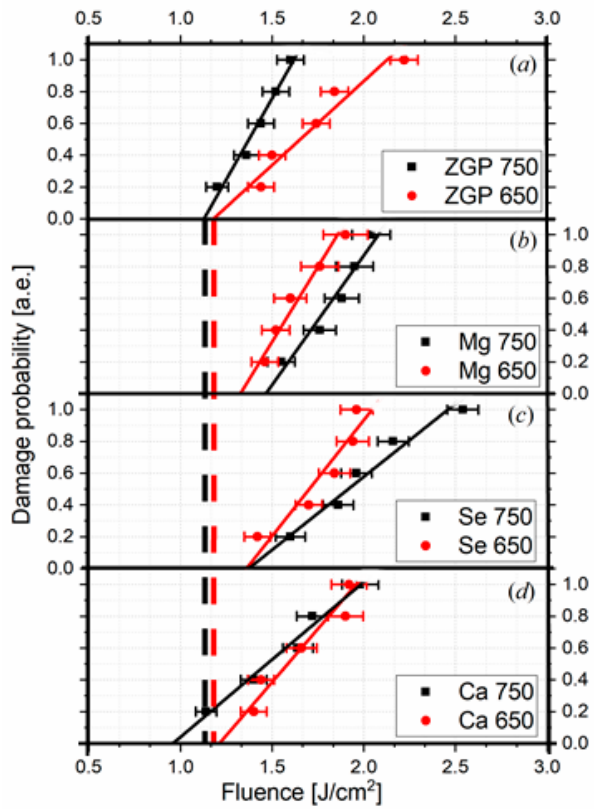

Figure 2. Dependence of the probability of optical damage on the energy density of the incident laser radiation with a wavelength of 2.1 μm in undoped samples (**a**) and in doped samples with Mg (**b**), Se (**c**), and Ca (**d**). Approximate plots in black and red correspond to ZGP samples annealed at 750 °C and 650 °C, respectively.

In the undoped samples (Figure 2a), there were no significant changes in the optical damage threshold (the detected changes were within the measurement error) depending on the annealing temperature, which corresponds to the results of [17]. At the same time, in the samples doped with magnesium and selenium by diffusion, after annealing at a temperature of 650 °C, the optical damage threshold increased by 15% and 17%, respectively. When annealing at a temperature of 750 °C, the damage threshold of the samples doped with Mg and Se increased by 31% and 21%, respectively. An inverse dependence was observed for the sample doped with Ca. When annealing at a temperature of 650 °C, no changes in the damage threshold were found and when annealing at a temperature of 750 °C, the damage threshold decreased by 14%. The presented results indicate a qualitative tendency for the optical damage threshold to decrease or increase depending on the concentration of the doped material. It should be noted that for the samples doped with Mg and Se, there was a tendency for the LIDT to increase with increasing dopant concentration (since samples annealed at 750 °C have a higher optical damage threshold than samples annealed at 650 °C). An inverse dependence was observed for the samples doped with Ca by diffusion. The best results were the results of the single crystal ZGP doped with Mg at a temperature of 750 °C.

In most experiments (about 85% of the total number of measurements), optical damage started appearing at the exit surface of the sample forming a breakdown path ending at the entrance surface.

From the results of measuring the LIDT and electrical conductivity (Table 1), a qualitative dependence can be seen. Doping with chemical elements causing a decrease in the electrical conductivity of the samples (σ) leads to an increase in the LIDT and vice versa, doping with chemical elements causing an increase in the electrical conductivity of the samples leads to a decrease in the LIDT. For example, when ZGP is doped with calcium, σ increases by about an order of magnitude while when ZGP is doped with Mg and Se, on the contrary, σ decreases by about an order of magnitude.

Table 1. Conductivity and optical damage threshold of the studied samples.

Dopant	σ, 1/Ω·cm	Optical Damage Threshold during Annealing 650 °C, J/cm^2	Optical Damage Threshold during Annealing 750 °C, J/cm^2
Mg	$(5.42 \pm 0.01) \times 10^{-6}$	2.6 ± 0.1	2.9 ± 0.1
Se	$(4.16 \pm 0.01) \times 10^{-7}$	2.64 ± 0.1	2.7 ± 0.1
Ca	$(1.25 \pm 0.01) \times 10^{-5}$	2.28 ± 0.1	1.9 ± 0.1
ZGP	$(1.24 \pm 0.01) \times 10^{-6}$	2.26 ± 0.1	2.2 ± 0.1

From the presented data in Table 1, the diffusion-doping with various chemical elements leads to an increase or a decrease in the optical damage threshold.

Figure 3 shows the dependence of the absorption spectrum in ZGP samples on the wavelength. The single crystal element (monocrystal) without annealing (indicated by the number, 1, in Figure 3) has the highest absorption in the short-wave infrared region among all samples. The group of curves located in the center (indicated by the number, 2) of the figure corresponds to elements annealed at a temperature of 650 °C. It can be noticed that the curve of one of the samples is a little far from the absorption level of the group in the range of 750–1350 nm. It corresponds to the undoped ZGP element. The difference in the absorption spectrum in this case can be explained by the absence of absorption centers in the used impurities in this spectral range and as a consequence, by a decrease in absorption by the doped surface of the single crystal elements.

The group of curves indicated by the number, 3, in Figure 3 corresponds to the samples annealed at 750 °C. Noticeably, diffusion-doping does not significantly change the IR absorption spectrum of ZGP; except for the sample doped with Ca, there is a slight increase in the absorption spectrum in a range of approximately 740–880 nm. The obtained

result indicates that calcium, and not the defects of the single crystal, is responsible for the decrease in the radiation resistance of ZGP doped with Ca (Figure 2.)

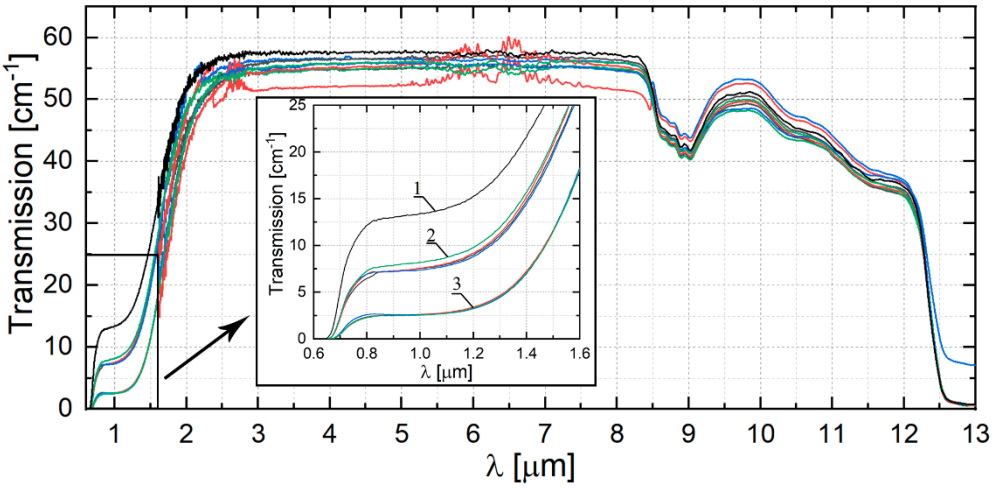

Figure 3. The dependences of the absorption coefficients for undoped and doped samples on the wavelength in the range of 0.6–12 μm at temperatures of 650 °C and 750 °C. Curve 1—sample after growth; group of curves 2—samples after annealing at a temperature of 650 °C; group of curves 3—samples after annealing at a temperature of 750 °C.

Optical damage in semiconductor materials at a nanosecond pulse duration of the acting laser radiation can be a consequence of thermal processes and processes associated with the generation of electron-hole plasma. It was suggested in [34] that there is a significant localized increase in temperature near small crystalline defects and inclusions under the action of pulsed radiation from a Ho:YAG laser, which leads to optical damage. Indeed, point-defects in a lattice of crystal enhance additional electronic sublevels, which lead to an increase in the multi-photon absorption at 2.09 μm and a sharp increase in temperature. A number of point-defects and inclusions accumulate in the dislocation regions located inside the ZGP, especially close to the surface, which leads to an increase in temperature to a critical value. On the other hand, the local electric field at the dislocation point is stronger than in a homogeneous lattice, which causes a decrease in the damage threshold enhanced by the electric field [16]. Thus, it becomes obvious that the decrease in the conductivity of ZGP doped with Mg and Se should lead to an increase in the optical damage threshold of ZGP crystals.

4. Effect of Dopants on the Quasi-Optical Properties of ZnGeP2 in the THz Range of the Spectrum

Absorption in the terahertz range was measured using a pulsed terahertz spectrometer in the time domain. The operating principle of this spectrometer is presented in detail in [34,35]. A Beam splitter plate (BS) is used to split a femtosecond laser radiation with a duration of 100 fs at a central wavelength of 780 nm, which using the Mai Tai SP laser (Spectra Physics, USA), generates a laser pulse in proportions of about 97% of the power to the pump beam and 3% of the power to probe beam. Terahertz pulses were generated in a GaSe crystal with a thickness, d, of 790 μm using the eee type of transformation [34,35]. An electro-optical ZnTe crystal with a thickness, d, of 1100 μm was used to detect the pulse passed through the studied ZGP sample.

According to [36], the absorption dispersion in ZGP in the range from 100 μm to 1000 μm monotonically decreases, and in a part of this range there is a non-fundamental absorption without resonances on the spectral curve.

It was shown in [37] by THz spectroscopy that the absorption of ZGP in the terahertz range of the spectrum (from 300 μm to 1000 μm) has a diffuse character; based on this fact,

the decisive role of free carriers in the formation of dielectric losses in this frequency range was assumed. This assumption was confirmed in [38] where it was indicated that one of the main sources of free carriers in ZGP is the interface between the matrix medium and the inclusion of the second phase. Since doping has an obvious effect on the conductivity of ZGP, it should have a significant effect on the absorption dispersion in the wavelength range (150–1000 μm).

The measurements of transmission of the studied sample in the terahertz spectrum (from 150 to 1000 μm), which were obtained using THz installation, allow for the calculation of the absorption coefficient. The measurement results of both doped samples using diffusion-doping and undoped samples annealed at temperatures of 650 °C and 750 °C are presented in Figure 4.

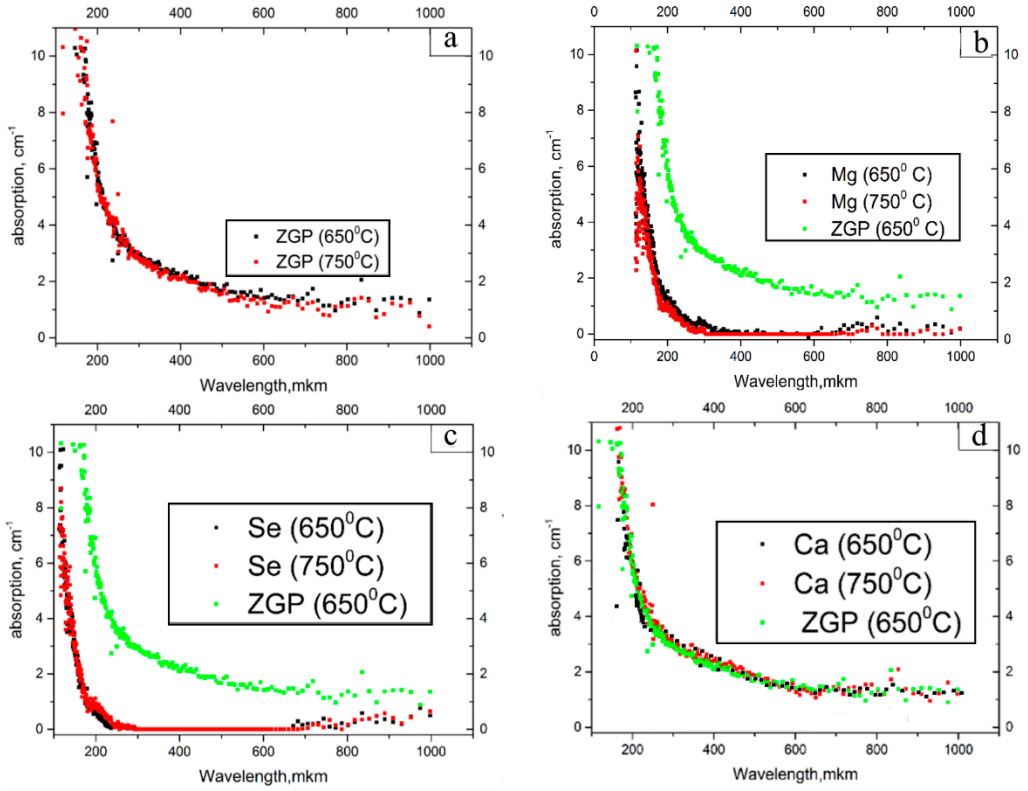

Figure 4. Dependence of linear absorption of ZGP samples on the wavelength in the THz range at annealing temperatures of 650 °C and 750 °C for 180 h (**a**), with diffusion-doping at temperatures of 650 °C and 750 °C with the following chemical elements: Mg (**b**), Se (**c**), Ca (**d**).

In the wavelength range of 150–1000 μm, the spectra of the absorption coefficient of samples doped with Mg, Se, and Ca were obtained, which are shown in Figure 4. From the obtained data, it can be seen that after doping the samples with Mg and Se atoms, a decrease in absorption is observed in the entire measured spectral range at annealing temperatures of 650 °C and 750 °C by ~1.5 cm^{-1}. After diffusion-doping with Ca atoms, no significant change in the absorption of the sample was revealed. As shown by the performed studies, the doped samples with Mg and Se exhibit a decrease in the specific conductivity in comparison with the undoped ZGP sample, which leads to a decrease in absorption in the THz range.

5. Conclusions

It is shown that the LIDT increases by diffusion-doping the ZGP single crystal with Mg and Se; upon annealing at a temperature of 750 °C, the damage threshold of samples doped with Mg and Se increases by 31% and 21% from 2.2 ± 0.1 J/cm^2 to 2.9 ± 0.1 and 2.7 ± 0.1 J/cm^2, respectively. When ZGP is doped with Ca, the opposite trend is observed.

A correlation is observed between the optical damage threshold and the electrophysical parameters of the crystals after doping, in particular with the conductivity of the samples. A decrease in conductivity is observed when the ZGP samples are doped with Mg and Se; when doped with Ca, the ZGP conductivity increases compared to the undoped annealed sample.

The conducted studies have shown that the technological possibility of increasing the LIDT of ZGP crystals can be achieved by reducing the conductivity of the samples by controlled doping.

The absorption spectra of the ZGP samples doped by diffusion with Mg, Se, and Ca atoms were measured in the THz range of the spectrum (100–1000 μm). The assumption that the absorption spectrum of ZGP in this range is determined by the concentration of free-charge carriers is confirmed. As shown by the performed studies, the samples doped with Mg and Se exhibit a decrease in specific conductivity compared to the undoped ZGP sample, which leads to a decrease in absorption in the THz range.

Author Contributions: Conceptualization, M.Z., N.Y. and S.P.; methodology, M.Z. and N.Y.; software, E.S., A.L. and H.B.; validation, A.K., E.S. and S.P.; formal analysis, N.Y. and M.Z.; investigation, N.Y., M.Z., S.P. and E.S.; resources, V.K. (Vera Kalygina); Data curation, V.V., L.S., E.S. and M.Z.; writing—original draft preparation, E.S.; writing—review and editing, N.Y., S.P. and H.B.; visualization, A.L. and V.K. (Vladimir Kuznetsov); supervision, N.Y. and M.Z.; project administration, M.Z. and N.Y.; funding acquisition, N.Y. All authors have read and agreed to the published version of the manuscript.

Funding: This study was supported by the Tomsk State University Development Program (Priority 2030).

Institutional Review Board Statement: Not applicable.

Conflicts of Interest: The authors declare no conflict of interest. The funders had no role in the design of the study; in the collection, analyses, or interpretation of the data; in the writing of the manuscript; and nor in the decision to publish the results.

References

1. Nikogosyan, D.N. *Nonlinear Optical Crystals: A Complete Survey*; Springer: New York, NY, USA, 2005; 427p.
2. Boyd, G.D.; Buehler, E.; Storz, F.G. Linear and nonlinear optical properties of $ZnGeP_2$ and CdSe. *Appl. Phys. Lett.* **1971**, *18*, 301–304. [CrossRef]
3. Dmitriev, V.G.; Gurzadyan, G.G.; Nikoghosyan, D.N. *Handbook of Nonlinear Optical Crystals*, 2nd ed.; Springer: Berlin, Germany, 1995; 160p.
4. Mason, P.D.; Jackson, D.J.; Gorton, E.K. CO_2 laser frequency doubling in $ZnGeP_2$. *Opt. Commun.* **1994**, *110*, 163. [CrossRef]
5. Vodopyanov, K.L.; Voevodin, V.G.; Gribenyukov, A.I.; Kulevsky, L.A. Owls. *J. Quantum Electron.* **1987**, *17*, 1159.
6. Henriksson, M.; Tiihonen, M.; Pasiskevicius, V.; Laurell, F. $ZnGeP_2$ parametric oscillator pumped by a line width narrowed parametric 2 μm source. *Opt. Lett.* **2006**, *31*, 1878–1880. [CrossRef] [PubMed]
7. Vodopyanov, K.L.; Ganikhanov, F.; Maffetone, J.P.; Zwieback, I.; Ruderman, W. $ZnGeP_2$ optical parametric oscillator with 3.8–12.4 μm tenability. *Opt. Lett.* **2000**, *25*, 841–843. [CrossRef] [PubMed]
8. Schunemann, P.G.; Zawilski, K.T.; Pomeranz, L.A.; Creeden, D.J.; Budni, P.A. Advances in nonlinear optical crystals for mid-infrared coherent sources. *J. Opt. Soc. Am. B* **2016**, *33*, D36–D43. [CrossRef]
9. Hemming, A.; Richards, J.; Davidson, A.A.; Carmody, N.; Bennetts, S.; Simakov, N.; Haub, J. 99 W mid-IR operation of a ZGP OPO at 25% duty cycle. *Opt. Express* **2013**, *21*, 10062–10069. [CrossRef] [PubMed]
10. Haakestad, M.W.; Fonnum, H.; Lippert, E. Mid-infrared source with 0.2 J pulse energy based on nonlinear conversion of Q-switched pulses in $ZnGeP_2$. *Opt. Express* **2014**, *22*, 8556–8564. [CrossRef]
11. Liu, G.; Mi, S.; Yang, K.; Wei, D.; Li, J.; Yao, B.; Yang, C.; Dai, T.; Duan, X.; Tian, L.; et al. 161 W middle infrared $ZnGeP_2$ MOPA system pumped by 300 W-class Ho:YAG MOPA system. *Opt. Lett.* **2021**, *46*, 82–85. [CrossRef]
12. Qian, C.; Yao, B.; Zhao, B.; Liu, G.; Duan, X.; Dai, T.; Ju, Y.; Wang, Y. High repetition rate 102 W middle infrared $ZnGeP_2$ master oscillator power amplifier system with thermal lens compensation. *Opt. Lett.* **2019**, *44*, 715–718. [CrossRef]
13. Wang, L.; Xing, T.; Hu, S.; Wu, X.; Wu, H.; Wang, J.; Jiang, H. Mid-infrared ZGP-OPO with a high optical-to-optical conversion efficiency of 75.7%. *Opt. Express* **2017**, *25*, 3373–3380. [CrossRef] [PubMed]
14. Wang, F.; Li, J.; Sun, X.; Yan, B.; Nie, H.; Li, X.; Yang, K.; Zhang, B.; He, J. High-power and high-efficiency 4.3 μm ZGP-OPO. *Chin. Opt. Lett.* **2022**, *20*, 011403. [CrossRef]
15. Medina, M.A.; Piotrowski, M.; Schellhorn, M.; Wagner, F.R.; Berrou, A.; Hildenbrand-Dhollande, A. Beam quality and efficiency of ns-pulsed high-power mid-IR ZGP OPOs compared in linear and non-planar ring resonators. *Opt. Express* **2021**, *29*, 21727–21737. [CrossRef] [PubMed]

16. Yudin, N.; Antipov, O.; Eranov, I.; Gribenyukov, A.; Verozubova, G.; Lei, Z.; Zinoviev, M.; Podzvalov, S.; Slyunko, E.; Voevodin, V.; et al. Laser-Induced Damage Threshold of Single Crystal $ZnGeP_2$ at 2.1 μm: The Effect of Crystal Lattice Quality at Various Pulse Widths and Repetition Rates. *Crystals* **2022**, *12*, 652. [CrossRef]
17. Yudin, N.N.; Antipov, O.L.; Gribenyukov, A.I.; Aronov, I.D.; Podzivalov, S.N.; Zinoviev, M.M.; Voronin, L.A.; Zhuravleva, E.V.; Zykova, M.P. Effect of postgrowth processing technology and laser radiation parameters at wavelengths of 2091 and 1064 nm on the laser-induced damage threshold in $ZnGeP_2$ single crystal. *Quantum Electron.* **2021**, *51*, 306–316. [CrossRef]
18. Zawilski, K.T.; Setzler, S.D.; Schunemann, P.G.; Pollak, T.M. Increasing the laser-induced damage threshold of single crystal $ZnGeP_2$. *J. Opt. Soc. Am. B* **2006**, *23*, 2310–2316. [CrossRef]
19. Yudin, N.; Khudoley, A.; Zinoviev, M.; Podzvalov, S.; Slyunko, E.; Zhuravleva, E.; Kulesh, M.; Gorodkin, G.; Kumeysha, P.; Antipov, O. The Influence of Angstrom-Scale Roughness on the Laser-Induced Damage Threshold of Single-Crystal $ZnGeP_2$. *Crystals* **2022**, *12*, 83. [CrossRef]
20. Peng, Y.; Wei, X.; Wang, W. Mid-infrared optical parametric oscillator based on $ZnGeP_2$ pumped by 2-μm laser. *Chin. Opt. Lett.* **2011**, *9*, 061403. [CrossRef]
21. Zinoviev, M.; Yudin, N.N.; Podzvalov, S.; Slyunko, E.; Yudin, N.A.; Kulesh, M.; Dorofeev, I.; Baalbaki, H. Optical AR Coatings of the Mid-IR Band for $ZnGeP_2$ Single Crystals Based on ZnS and Oxide Aluminum. *Crystals* **2022**, *12*, 1169. [CrossRef]
22. Zinovev, M.; Yudin, N.N.; Kinyaevskiy, I.; Podzyvalov, S.; Kuznetsov, V.; Slyunko, E.; Baalbaki, H.; Vlasov, D. Multispectral Anti-Reflection Coatings Based on YbF3/ZnS Materials on ZnGeP2 Substrate by the IBS Method for Mid-IR Laser Applications. *Crystals* **2022**, *12*, 1408. [CrossRef]
23. Yudin, N.N.; Zinoviev, M.; Gladkiy, V.; Moskvichev, E.; Kinyaevsky, I.; Podzyvalov, S.; Slyunko, E.; Zhuravleva, E.; Pfaf, A.; Yudin, N.A.; et al. Influence of the Characteristics of Multilayer Interference Antireflection Coatings Based on Nb, Si, and Al Oxides on the Laser-Induced Damage Threshold of ZnGeP2 Single Crystal. *Crystals* **2021**, *11*, 1549. [CrossRef]
24. Gribenyukov, A.I.; Dyomin, V.V.; Olshukov, A.S.; Podzyvalov, S.N.; Polovtsev, I.G.; Yudin, N.N. Investigation of the process of optical damage of $ZnGeP_2$ crystals using digital holography. *Rus. Phys. J.* **2019**, *61*, 2042–2052. [CrossRef]
25. Dyomin, V.V.; Gribenyukov, A.I.; Davydova, A.Y.; Olshukov, A.S.; Polovtsev, I.G.; Podzyvalov, S.N.; Yudin, N.N.; Zinovev, M.M. Visualization of volumetric defects and dynamic processes in crystals by digital IR-holography. *Appl. Opt.* **2021**, *60*, A296–A305. [CrossRef] [PubMed]
26. Guo, J.; Xie, J.; Li, D.; Yang, G.; Chen, F.; Wang, C.; Zhang, L.; Andreev, Y.; Kokh, K.; Lanskii, G.; et al. Doped GaSe crystals for laser frequency conversion. *Light: Sci. Appl.* **2015**, *4*, e362. [CrossRef]
27. Liu, L.; Chen, F.; Cui, J.; Xiao, X.; Xu, Y.; Hou, C.; Cui, X.; Guo, H. The mutual influence between rare earth element doping and femtosecond laser-induced effects in Ga-As-Sb-S chalcogenide glass. *Ceram. Int.* **2021**, *47*, 6388–6396. [CrossRef]
28. Bussière, B.; Utéza, O.; Sanner, N.; Sentis, M.; Riboulet, G.; Vigroux, L.; Commandré, M.; Wagner, F.; Natoli, J.-Y.; Chambare, J.-P. Bulk laser-induced damage threshold of titanium-doped sapphire crystals. *Appl. Opt.* **2012**, *51*, 7826–7833. [CrossRef] [PubMed]
29. Voevodin, V.G.; Chaldyshev, V.A. Study of ternary semiconductors $A_2B_4C_5$. *Bull. Tomsk. State Univ.* **2005**, *285*, 63–73.
30. Voevodin, V.G. *Elements of Optical Electronics Based on Compounds $A_2B_4C_5$: Obtaining, Properties and Application: Dissertation of the Doctor of Physical and Mathematical Sciences: 01.04.05, 01.04.10*; Tomsk State University: Tomsk, Russia, 2003; 395p.
31. *ISO11146-1:2005*; Lasers and Laser-Related Equipment—Test Methods for Laser Beam Widths, Divergence Angles and Beam Propagation Ratios—Part 1: Stigmatic and Simple Astigmatic Beams. ISO: Geneva, Switzerland, 2005.
32. The R-on-1 Test. Lidaris LIDT Service. 2019. Available online: https://lidaris.com/laser-damage-testing/r-on-1-test/ (accessed on 30 September 2022).
33. Ramadan, A.A.; Gould, R.D.; Ashour, A. On the Van der Pauw method of resistivity measurements. *Thin Solid Film.* **1994**, *239*, 272–275. [CrossRef]
34. Nazarov, M.M.; Sarkisov, S.Y.; Shkurinov, A.P.; Tolbanov, O.P. $GaSe_{1-x}S_x$ and $GaSe_{1-x}Te_x$ thick crystals for broadband terahertz pulses generation. *Appl. Phys. Lett.* **2011**, *99*, 081105. [CrossRef]
35. Bereznaya, S.A.; Korotchenko, Z.V.; Redkin, R.A. Broadband and narrowband terahertz generation and detection in $GaSe_{1-x}S_x$ crystals Creator. *J. Opt.* **2017**, *19*, 115503. [CrossRef]
36. Chuchupal, S.V.; Komandin, G.A.; Zhukova, E.S.; Prokhorov, A.S.; Porodinkov, O.E.; Spektor, I.E.; Shakir, Y.A.; Gribenyukov, A.I. Mechanisms of Loss Formation in Nonlinear Optical Crystals $ZnGeP_2$ in the Terahertz Frequency Range. *Phys. Solid State* **2014**, *56*, 1391–1396. [CrossRef]
37. Chuchupal, S.V.; Komandin, G.A.; Zhukova, E.S.; Porodinkov, O.E.; Spektor, I.E.; Gribenyukov, A.I. Effect of electron irradiation of ZnGeP2 single crystals on terahertz losses in a wide temperature range. *Phys. Solid State* **2015**, *57*, 1607–1612. [CrossRef]
38. Zinoviev, M.; Yudin, N.; Gribenyukov, A.; Podzyvalov, S.; Dyomin, V.; Polovtsev, I.; Suslyaev, V.; Zhuravlyova, Y. The effect of volume inclusions of the ZnGeP2 single-crystal on the dispersion of the refraction index and the absorption coefficient in mid-IR and terahertz ranges of wavelengths. *Opt. Mater.* **2021**, *111*, 110662. [CrossRef]